Technical Note

Reproducibility of Flow and Wall Shear Stress Analysis Using Flow-Sensitive Four-Dimensional MRI

Michael Markl, PhD,[1]* Wolf Wallis, MD,[2] and Andreas Harloff, MD[2]

Purpose: To systematically investigate the scan–rescan reproducibility and observer variability of flow-sensitive four-dimensional (4D) MRI in the aorta for the assessment of blood flow and global and segmental wall shear stress.

Materials and Methods: ECG and respiration-synchronized flow-sensitive 4D MRI data (spatio-temporal resolution = $1.7 \times 2.0 \times 2.2$ mm^3/40.8 ms) were acquired in 12 healthy volunteers. To analyze scan–rescan variability, flow-sensitive 4D MRI was repeated in 10 volunteers during a second visit. Data analysis included calculation of time-resolved and total flow, peak systolic velocity, and regional and global wall shear stress (WSS) in up to 24 analysis planes distributed along the aorta.

Results: Scan–rescan, inter-observer, and intra-observer agreement was excellent for the calculation of total flow and peak systolic velocity (mean differences <5% of the average flow parameter). Global WSS demonstrated moderate agreement and increased variability regarding wall shear stress (scan-rescan, inter-observer, and intra-observer agreement; mean differences <10% of the average WSS parameters). The segmental distribution of wall shear stress in the thoracic aorta could reliably be reproduced ($r > 0.87$; $P < 0.001$) for different observers and examinations.

Conclusion: Flow-sensitive 4D MRI-based analysis of aortic blood flow can be performed with good reproducibility. Robustness of global and regional WSS quantification was limited, but spatio-temporal WSS distributions could reliably be replicated.

Key Words: flow-sensitive MRI; phase contrast; blood flow; 4D flow; wall shear stress; aorta
J. Magn. Reson. Imaging 2011;33:988–994.
© 2011 Wiley-Liss, Inc.

TIME-RESOLVED (CINE) phase-contrast (PC) MRI has been widely used for the assessment of in vivo blood flow (1,2). In recent years, the quantitative analysis of blood flow characteristics within the entire thoracic aorta using time-resolved PC MRI with three-directional velocity encoding and three-dimensional (3D) anatomic coverage (flow-sensitive 4D MRI) has gained increased importance (3–5). These techniques can be applied both for the visualization of complex 3D blood flow characteristics (6–8) and for the quantification of regional blood flow and derived parameters such as wall shear stress (WSS) (9–11), pressure differences (12,13), or turbulent kinetic energy (14). Recently, this technique has been used to evaluate the distribution of wall shear stress in the aorta of healthy volunteers (15), and initial reports on altered WSS in the presence of disease have been presented (16,17).

The accuracy, reproducibility, and observer dependence of such methods determine their potential in clinical applications. Blood flow quantification using standard CINE 2D PC MRI has been extensively validated in the past. Previous studies demonstrated its potential for accurate ventricular stroke volume measurements in vitro and in vivo (18,19) and for reliable flow quantification in the aorta and pulmonary system compared with Doppler ultrasound (20,21). Other studies found high reproducibility for 2D PC MRI flow quantification in the pulmonary venous system and in a pulsatile flow phantom (22,23) as well as low intra- and inter-observer variation for quantifying the transvalvular flow through the mitral valve (24).

There are only a few reports on the reliability of WSS estimation from PC MRI data using software phantoms, in vitro flow experiments, or computational fluid dynamics (CFD) (16,25,26).

Although the performance of flow and wall parameter estimation based on flow-sensitive 4D MRI has been compared with standard 2D PC MRI (11,27), a detailed analysis of the scan-rescan reproducibility as well as its inter- and intra-observer dependence associated with the retrospective definition of analysis planes and vessel lumen segmentation is still missing.

It was the aim of this study to systematically investigate these potential confounders for typically assessed clinical flow parameters such as total flow

[1]Department of Radiology - Medical Physics, University Hospital Freiburg, Germany.
[2]Department of Neurology, University Hospital Freiburg, Germany.
Contract grant sponsor: Bundesministerium für Bildung und Forschung; Contract grant number: 01EV0706.
*Address reprint requests to: M.M., University Hospital Freiburg, Department of Radiology, Medical Physics, Breisacher Strasse 60a, 79106 Freiburg, Germany. E-mail: michael.markl@uniklinik-freiburg.de
Received May 10, 2010; Accepted January 13, 2011.
DOI 10.1002/jmri.22519
View this article online at wileyonlinelibrary.com.

© 2011 Wiley-Liss, Inc.

Table 1
Demographics of the Volunteer Cohort and the Subgroup Undergoing Repeated Flow-Sensitive 4D MRI of the Aorta

	Entire study (observer agreement)	Reproducibility study		Paired t-test (scan 1 vs. scan 2)
	population	Scan 1	Scan 2	*P* value
Number	12	10	10	-
Heart rate [bpm]	66 ± 9	65 ± 9	62 ± 8	0.34
RR sys [mmHg]	130 ± 15	130 ± 14	129 ±12	0.81
RR dia [mmHg]	83 ± 12	82 ± 11	75 ± 12	0.21

bpm =beats per minute; RR sys = systolic blood pressure; RR dia = diastolic blood pressure.

(estimation of stroke volume) and peak systolic velocity (estimation of pressure gradients across stenosis by the simplified Bernoulli equation). Moreover, the reproducibility of global and regional wall shear stress estimation from flow-sensitive 4D MR data was investigated.

MATERIALS AND METHODS

Study Population

Between April and July 2008, 12 healthy volunteers were included in the study. In 10 subjects, flow-sensitive 4D MRI was repeated during a second visit 1 year later (June and August 2009). Volunteers' demographics are summarized in Table 1. The study was approved by our local ethics board and written informed consent was obtained from all participants.

MR Imaging

All experiments were conducted on a 3 Tesla (T) MR system (TRIO, Siemens, Germany) equipped with a standard 12-element torso coil. For evaluation of blood flow and wall parameters, time-resolved 3D PC MRI with three-directional velocity encoding (flow-sensitive 4D MRI) was used. ECG-synchronized (prospective gating) and respiration-controlled (navigator gating of the lung-liver interface) flow-sensitive MRI was executed using a sagittal oblique 3D volume covering the entire thoracic aorta as described previously (4). The scan parameters were as follows: echo time/repetition time (TE/TR) = 2.6 ms/5.1 ms, flip angle = 7°, temporal resolution = 40.8 ms, matrix size = 192 × 120 × 26, bandwidth = 450 Hz/pixel, spatial resolution = 1.7 × 2.0 × 2.2 mm^3, velocity sensitivity along all three directions = 150 cm/s, parallel imaging (GRAPPA) along phase encoding direction (y) with reduction factor R = 2 (24 reference lines). No parallel imaging was applied for the slice encoding direction (z). The total scan time for flow-sensitive 4D MRI ranged between 12–20 min, depending on heart rate and respiratory gating efficiency.

Hemodynamic Monitoring

After a minimum of 5 min in a supine position, systolic and diastolic blood pressures were measured at the volunteer's right upper arm before the scan, and this was repeated at the end of the MRI scan. In addition, heart rate was taken every 4 min during the MRI session.

Data Analysis

Flow-sensitive 4D MRI data underwent corrections for concomitant gradient fields, eddy currents, and velocity aliasing as previously described (28–30). Noise masking and subsequent calculation of absolute blood flow velocities weighted by the magnitude data permitted the calculation of a time-averaged 3D phase contrast angiography (PC-MRA) dataset. The 3D PC-MRA was used to manually position analysis planes in the ascending aorta, arch, and proximal descending aorta using a 3D visualization software (EnSight, CEI, USA) (4). To provide comparable analysis plane locations all planes were systematically distributed across the thoracic aorta according to the following scheme: An initial analysis plane was positioned directly distal to the outlet of the left subclavian artery. All other 2D analysis planes were positioned upstream and downstream with a distance of 10 mm between adjacent planes. Consistent inter-plane distance was achieved by using a software functionality which allowed to automatically move the plane position by 10 mm along the normal vector of the analysis plane. The position of each plane was angulated orthogonal to the aortic lumen. The analysis planes covered the aorta from the proximal ascending aorta to descending aorta at the height of the pulmonary artery.

For each analysis plane, the aortic lumen contours were manually drawn for all time-frames using a home built tool programmed in Matlab (Matlab, The Mathworks, USA), and flow–time curves, total flow, and peak systolic velocity were calculated.

Wall shear stress (WSS) estimation was based on a direct interpolation of the local velocity derivative on the segmented vessel lumen contour using b-splines as described previously (11). Based on a consistent orientation of the analysis planes, regional time-resolved WSS vectors could be mapped onto a standardized four-quadrant model representing four angular segments of the aortic wall (inner curvature, outer curvature, left side, right side). Segmental time-averaged and absolute WSS (i.e., the lengths of the WSS vectors) was averaged over all subjects and mapped onto a bulls-eye plot to visualize its distribution in the entire aorta.

Global WSS (spatially averaged along the aortic lumen) was investigated by calculating the temporal evolution of absolute WSS over the cardiac cycle, time-averaged absolute wall shear stress (<WSS>), and peak systolic wall shear stress (WSS_{peak}).

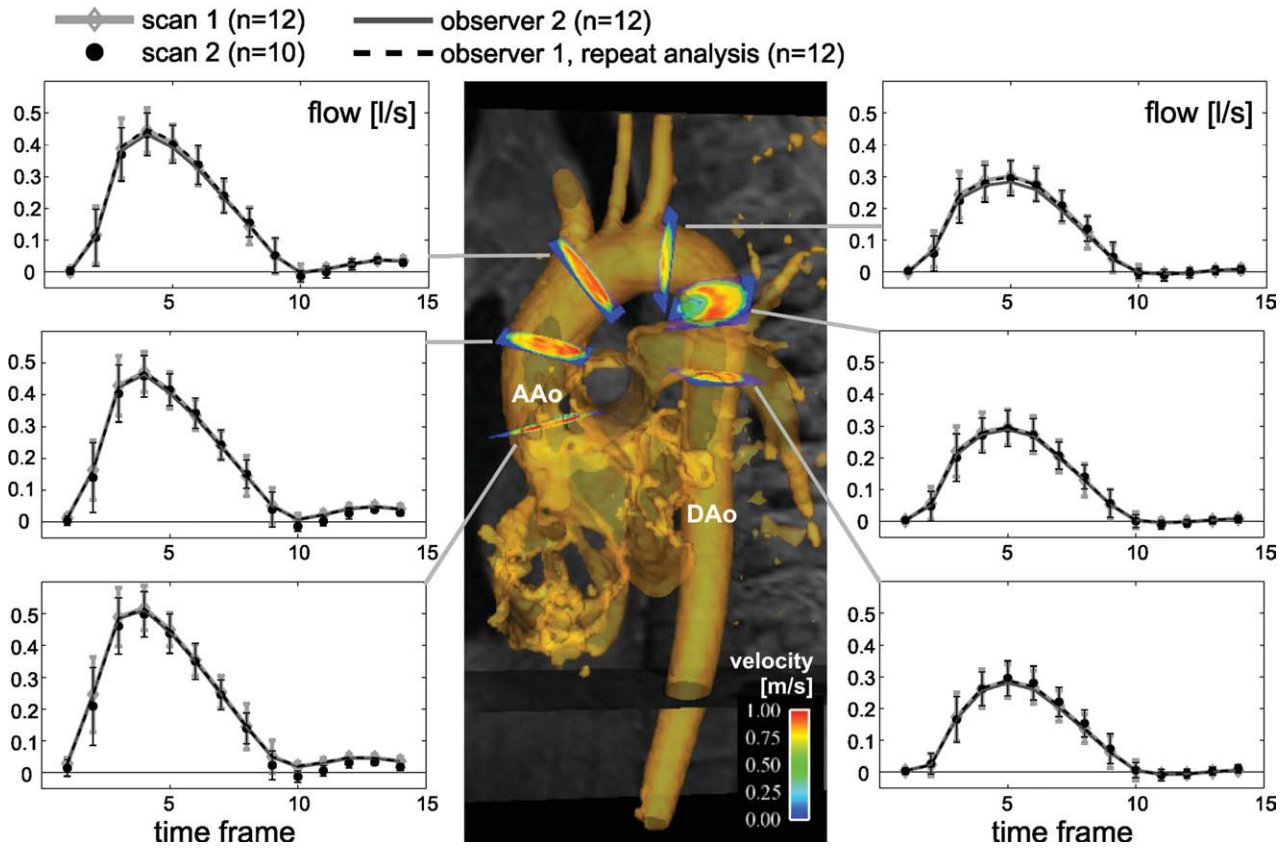

Figure 1. Pulsatile aortic blood flow curves distributed across the thoracic aorta. Error bars reflect inter-individual standard deviations of flow among n = 12 subjects for scan 1 and n = 10 volunteers for scan 2. Standard deviations for inter- and intra-observer agreement were similar (not shown for better visibility of the results).

Inter- and intra-observer analysis

All analysis planes along the aorta were positioned by observer 1. For the analysis of inter-observer variability, the lumen segmentation for all analysis planes and 12 volunteers (254 analysis planes) was repeated by a second observer who was blinded to the results by observer 1. For the analysis of intra-observer variability, observer 1 repeated the lumen segmentation of all aortic analysis planes in 12 volunteers.

Scan–Rescan variability

For the analysis of scan–rescan reproducibility data from 10 volunteers form measurements during the first visit (scan 1) and the second visit (scan 2) were analyzed by observer 1 (positioning of a total of 2 × 211 analysis planes and frame-wise lumen segmentation for each plane).

Statistical Analysis

Continuous variables are reported as mean ± standard deviation. Reproducibility, inter- and intra-observer agreement were evaluated using the approach by Bland-Altman (31) by calculating the mean difference (d) and standard deviation (σ) of the difference. From these data, the limits of agreement (± 2σ) were calculated (95% confidence intervals). For Bland Altman comparisons, data from all subjects and analysis planes were compared. To compare planar blood flow and wall shear stress parameters as well as the distribution of segmental WSS, correlation analysis based on linear regression was used. The overall quality of the regression was assessed using Pearson's correlation coefficient r; a correlation was considered significant for $P < 0.05$. To detect statistically significant differences between continuous variables, paired t-tests were applied.

RESULTS

Different aortic sizes resulted in the placement of 21 ± 2 (range, 19–24) analysis planes in the individual vessel. Nineteen analysis planes were common to all volunteers.

Blood Flow

Plane by plane comparison of flow–time curves between repeated scans and between the two observers showed good agreement as illustrated for six selected analysis planes in Figure 1. Similarly, Bland-Altman analysis (Table 2; Fig. 2) demonstrated only small variations for total flow (scan rescan and observer mean differences < 5% of the average total flow) and peak systolic velocities (mean differences < 3% of the average peak velocity). Correlation analysis

Table 2
Results of the Bland and Altman and Correlation Analysis of Reproducibility as Well as of Inter- and Intra-observer Variability for the Calculation of Planar Blood Flow and Wall Shear Stress Parameters

	Descriptive	Reproducibility (scan 1 vs. scan 2)				Inter-observer variability				Intra-observer variability			
	statistics	Bland-Altman		Correlation		Bland-Altman		Correlation		Bland-Altman		Correlation	
	mean ± SD (min-max)	d	ςd	r	*P* value	d	ςd	r	*P* value	d	ςd	r	*P* value
Total flow [ml/cycle]	83 ± 25 (42-142)	−4	±20	0.92	<0.001	−2	±5	0.99	<0.001	0	±3	0.99	<0.001
peak flow [ml/s]	397 ± 121 (196-669)	−6	±72	0.95	<0.001	−8	±23	0.99	<0.001	−1	±15	0.99	<0.001
<WSS> [N/m^2]	0.32 ± 0.08 (0.10-0.58)	−0.03	±0.14	0.55	<0.001	−0.02	±0.09	0.84	<0.001	0	±0.07	0.87	<0.001
WSS_{peak} [N/m^2]	1.00 ± 0.21 (0.29-1.61)	−0.09	± 0.40	0.59	<0.001	-0.04	±0.26	0.80	<0.001	−0.01	±0.23	0.82	<0.001

d = mean difference, σd = limits of agreement; r = correlation coefficient.

confirmed significant ($P < 0.001$) and high ($r \geq 0.92$) correlations for reproducibility and inter- and intra-observer agreement (Table 2).

Wall Shear Stress

As summarized in Table 2, plane-wise calculation of <WSS> and WSS_{peak} demonstrated significant agreement ($r \geq 0.55$; $P < 0.001$) for reproducibility and good performance for inter- and intra-observer agreement ($r \geq 0.80$, $P < 0.001$). Compared with the blood flow parameters, Bland-Altman analysis revealed increased scan–rescan, inter-observer, and intra-observer variability for time-averaged absolute WSS (scan rescan and observer mean differences < 10% of the average <WSS>) and peak systolic WSS (mean differences < 9% of the average WSS_{peak}). Nevertheless, the time-resolved evolution of plane-wise WSS over the cardiac cycle showed close agreement between repeated scans and between the two observers as illustrated in Figure 3 for six selected analysis planes.

The results of the segmental wall shear stress analysis are illustrated in Figure 4. It is evident that different scans and observers resulted in variations in time-averaged absolute <WSS> values (gray scale level in bulls-eye plots). Nevertheless, the relative distribution of segmental <WSS>, e.g., relative low

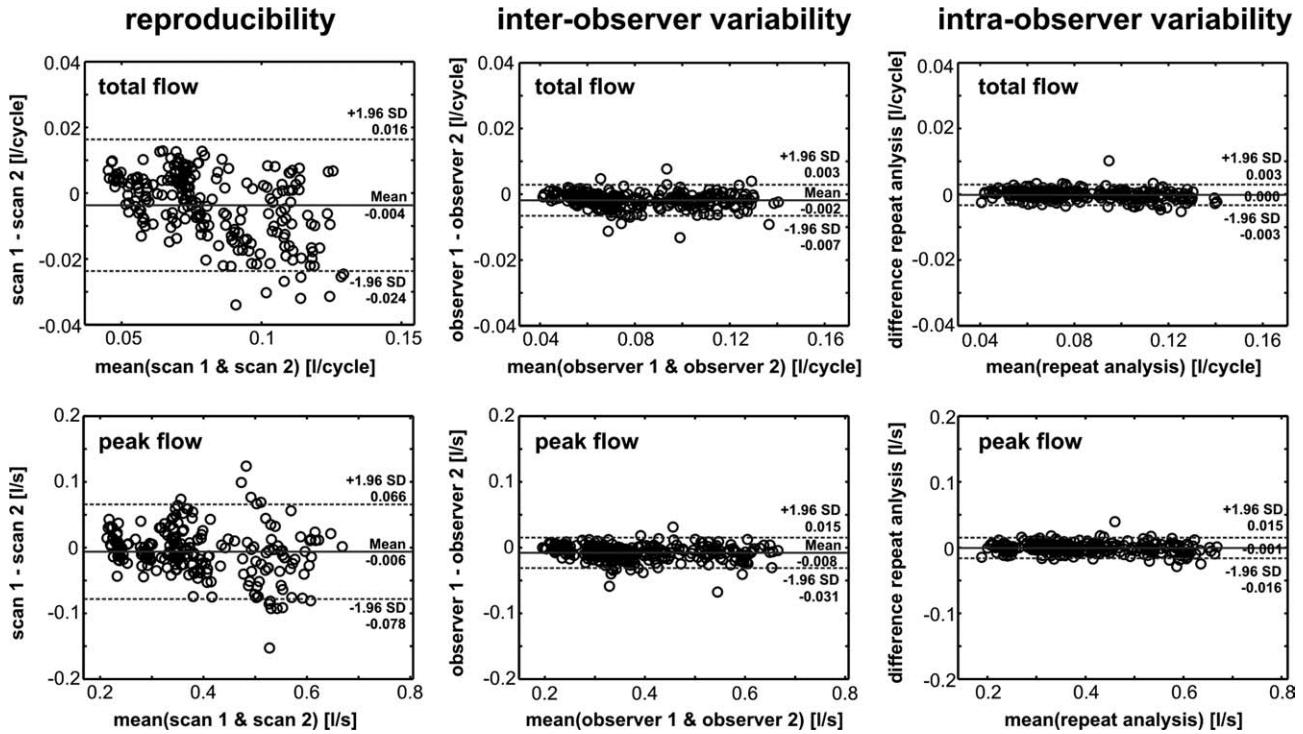

Figure 2. Bland and Altman analysis of reproducibility (scan–rescan variability) and of inter-and intra-observer agreement for flow parameter calculation in the thoracic aorta.

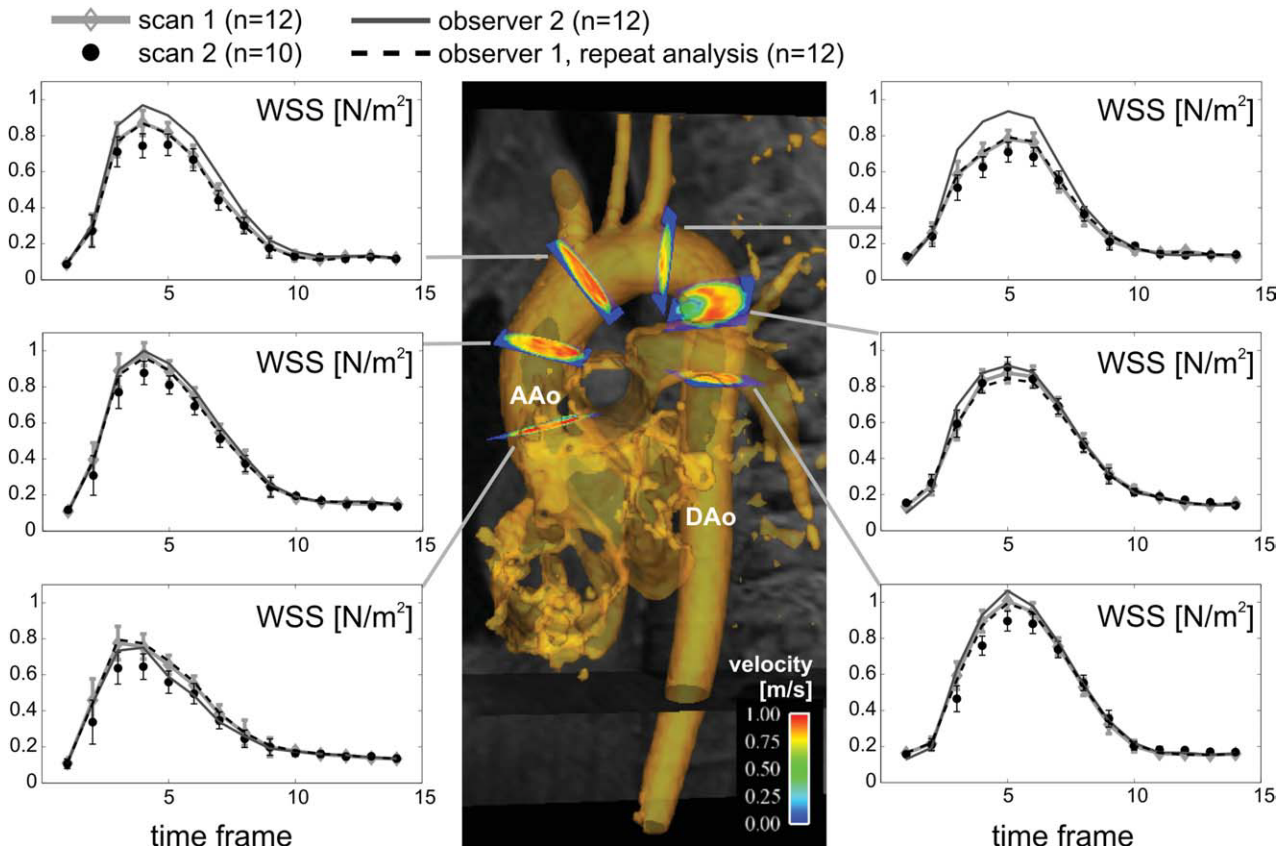

Figure 3. Time-resolved WSS in different analysis planes distributed along the thoracic aorta. Error bars reflect inter-individual standard deviations of wall parameters among n = 12 subjects for scan 1 and n = 10 volunteers for scan 2. Standard deviations for inter- and intra-observer variability were similar (not shown for better visibility of the results).

<WSS> at the left inner curvature of the ascending aorta or at the inner wall of the proximal descending aorta, was consistent for different observers and examinations. Results of linear regression analysis verified a significant ($P < 0.001$) correlation between distributions for scan–rescan (r = 0.87), inter-observer ($r = 0.88$), and intra-observer ($r = 0.97$) comparisons.

DISCUSSION

Scan–rescan, inter-, and intra-observer comparisons of quantitative aortic flow-sensitive 4D MRI revealed good robustness (<5% variation compared with average values) for the calculation of standard blood flow parameters such as total flow and systolic peak velocities. We believe that these variations are acceptable for typical clinical applications which rely on integrated flow time curves (stroke volume, regurgitant flow) or measurement of peak velocities (stenosis grading).

Estimation of global wall shear stress demonstrated reduced and moderate reproducibility (<10% variation compared with average values) and wider limits of agreement. Based on our current data analysis strategy, it may thus be problematic to rely on absolute wall shear stress values. Nevertheless, the relative distribution of segmental wall parameters was consistent and could serve as a valuable tool to identify areas with altered wall parameters compared with other vascular regions and thus risk for vascular remodeling.

One of the major drawbacks of the current data analysis strategy is related to the manual delineation of vessel lumen boundaries which can introduce operator dependent variations in segmentation contours. The calculation of blood flow, which showed only small variability, is relatively independent from such inaccuracies. Low or zero velocity components missed or added due to segmentation errors will lead to only small errors since flow = mean velocity within the lumen * lumen area. In contrast, WSS estimation was based on the calculation of the local velocity derivative at the vessel lumen boundary and is thus more sensitive to the definition of the segmentation contour (11,15).

Analysis by observer 2 (Figs. 1, 2; gray lines) consistently resulted in higher values for WSS. It is likely that observer 1 drew lumen boundaries closer to the vessel center thereby increasing the velocity gradient and thus WSS. This observer-dependency should be eliminated in future studies by the introduction of semi- or fully automated segmentation methods (19) into the data processing chain.

For both blood flow and wall parameters, the highest variability was observed for the scan–rescan analysis. Although heart rate and blood pressure were not significantly different between scan 1 and scan 2 (see Table 1), we hypothesize that changes in hemodynamic

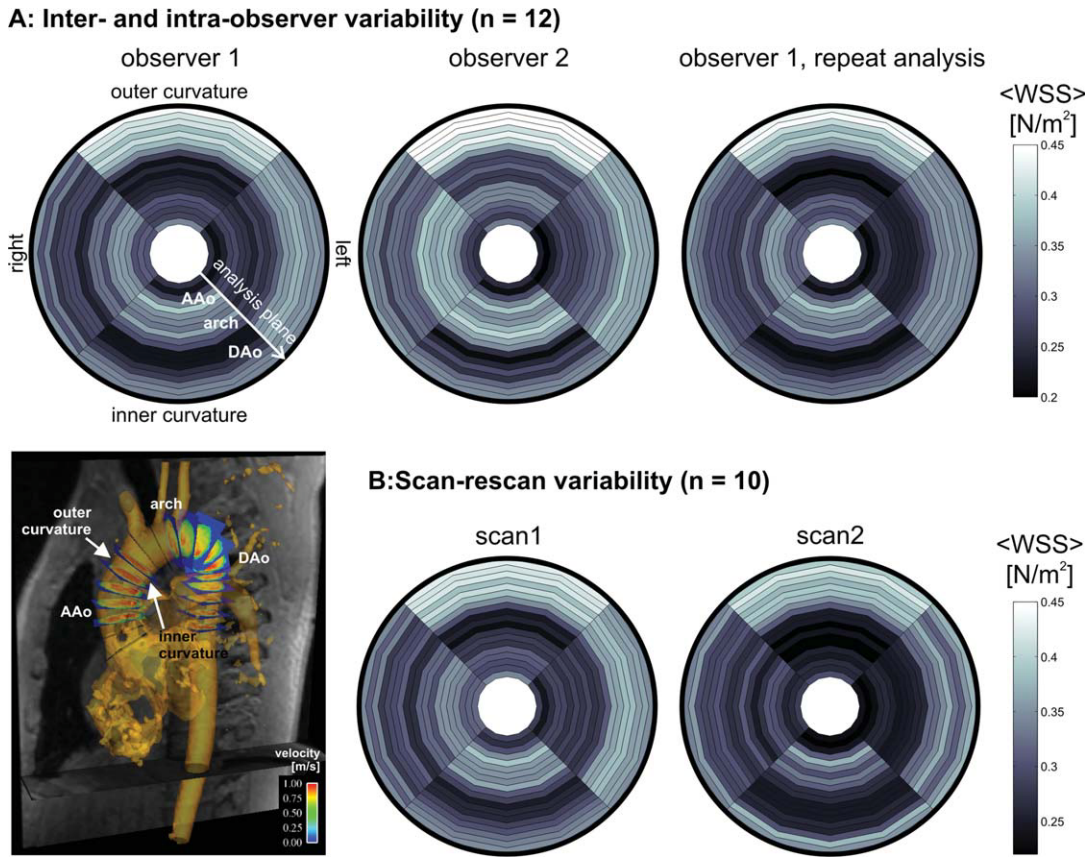

Figure 4. Inter- and intra-observer variability (**A**) and scan–rescan variability (**B**) of the segmental wall shear stress distribution in the normal thoracic aorta. The bulls-eye plots represent the regional distribution of <WSS> in 4 segments of the aortic wall for 19 equidistant analysis planes common to all volunteers: Analysis planes were consistently distributed along the ascending aorta (AAo), aortic arch, and descending aorta (DAo) as shown in the lower left panel. The gray scale in the individual segments represents average <WSS> over 12 subjects for inter- and intra-observer variability (A) and over 10 volunteers for scan–rescan variability (B).

parameters and the long time between scan and rescan may have elevated variability.

It should be noted that the findings of this study are based on intra-modality comparisons and no gold standard was used to evaluate the accuracy of flow parameter and wall shear stress analysis. Previous studies used numerical blood flow simulations (computational fluid dynamics, CFD) or in vitro model systems to validate flow quantification and WSS estimation (25,26). Similar to the findings in this study, recent work by Boussel et al (16) comparing MRI and CFD found that flow-sensitive 4D MRI accurately measured velocity flow fields but was limited regarding the accurate quantification of wall shear stress. However, both CFD and in vitro systems are limited by model assumptions, or simplified vascular geometry. To our knowledge, there exists currently no imaging modality that could be considered a gold standard for the in vivo assessment of wall shear stress.

Note that absolute WSS (lengths of the WSS vector) and not axial WSS (projection of the WSS vector along the lumen direction) was used for the analysis in this work. While it is still unclear which WSS component can provide the most sensitive marker for altered vessel function, we believe that axial WSS may underestimate the true WSS magnitude in the presence of non-axial (circumferential) WSS components. For example, in a previous study (15), we could show the existence of circumferential WSS component in young normal volunteers, indicating the importance to consider the full spatial variation of WSS rather than merely the axial component.

The investigated scan–rescan reproducibility was a best-case scenario with both scans being performed on the same type of MR system with exactly the same imaging protocol. Incorporating another scanner type or varying the spatio-temporal resolution may have resulted in altered reproducibility, which should be investigated in more detail in future studies. In addition, findings in larger numbers of patients showing a higher variability of aortic anatomy and/or hemodynamics should be performed to further evaluate the robustness of this method for clinical use.

In conclusion, analysis of standard flow parameters using aortic flow-sensitive 4D MRI in normal volunteers can be performed with low variability. The reproducibility for quantification of global and regional WSS was limited but relative spatio-temporal WSS distributions could reliably be replicated. A more automated analysis of 3D flow data has the potential to improve robustness and may allow its wider clinical application.

REFERENCES

1. Moran PR. A flow velocity zeugmatographic interlace for NMR imaging in humans. Magn Reson Imaging 1982;1:197–203.
2. Firmin DN, Nayler GL, Kilner PJ, Longmore DB. The application of phase shifts in NMR for flow measurement. Magn Reson Med 1990;14:230–241.
3. Wigstrom L, Sjoqvist L, Wranne B. Temporally resolved 3D phase-contrast imaging. Magn Reson Med 1996;36:800–803.
4. Markl M, Harloff A, Bley TA, et al. Time-resolved 3D MR velocity mapping at 3T: improved navigator-gated assessment of vascular anatomy and blood flow. J Magn Reson Imaging 2007;25:824–831.
5. Hope TA, Herfkens RJ. Imaging of the thoracic aorta with time-resolved three-dimensional phase-contrast MRI: a review. Semin Thorac Cardiovasc Surg 2008;20:358–364.
6. Bogren HG, Buonocore MH, Valente RJ. Four-dimensional magnetic resonance velocity mapping of blood flow patterns in the aorta in patients with atherosclerotic coronary artery disease compared to age-matched normal subjects. J Magn Reson Imaging 2004;19:417–427.
7. Buonocore MH. Visualizing blood flow patterns using streamlines, arrows, and particle paths. Magn Reson Med 1998;40:210–226.
8. Kozerke S, Hasenkam JM, Pedersen EM, Boesiger P. Visualization of flow patterns distal to aortic valve prostheses in humans using a fast approach for cine 3D velocity mapping. J Magn Reson Imaging 2001;13:690–698.
9. Oshinski JN, Ku DN, Mukundan S Jr, Loth F, Pettigrew RI. Determination of wall shear stress in the aorta with the use of MR phase velocity mapping. J Magn Reson Imaging 1995;5:640–647.
10. Oyre S, Pedersen EM, Ringgaard S, Boesiger P, Paaske WP. In vivo wall shear stress measured by magnetic resonance velocity mapping in the normal human abdominal aorta. Eur J Vasc Endovasc Surg 1997;13:263–271.
11. Stalder AF, Russe MF, Frydrychowicz A, Bock J, Hennig J, Markl M. Quantitative 2D and 3D phase contrast MRI: optimized analysis of blood flow and vessel wall parameters. Magn Reson Med 2008;60:1218–1231.
12. Tyszka JM, Laidlaw DH, Asa JW, Silverman JM. Three-dimensional, time-resolved (4D) relative pressure mapping using magnetic resonance imaging. J Magn Reson Imaging 2000;12:321–329.
13. Ebbers T, Wigstrom L, Bolger AF, Wranne B, Karlsson M. Noninvasive measurement of time-varying three-dimensional relative pressure fields within the human heart. J Biomech Eng 2002; 124:288–293.
14. Dyverfeldt P, Sigfridsson A, Kvitting JP, Ebbers T. Quantification of intravoxel velocity standard deviation and turbulence intensity by generalizing phase-contrast MRI. Magn Reson Med 2006;56: 850–858.
15. Frydrychowicz A, Stalder AF, Russe MF, et al. Three-dimensional analysis of segmental wall shear stress in the aorta by flow-sensitive four-dimensional-MRI. J Magn Reson Imaging 2009;30: 77–84.
16. Boussel L, Rayz V, Martin A, et al. Phase-contrast magnetic resonance imaging measurements in intracranial aneurysms in vivo of flow patterns, velocity fields, and wall shear stress: comparison with computational fluid dynamics. Magn Reson Med 2009;61: 409–417.
17. Harloff A, Nussbaumer A, Bauer S, et al. In vivo assessment of wall shear stress in the atherosclerotic aorta using flow-sensitive 4D MRI. Magn Reson Med 2010;63:1529–1536.
18. Firmin DN, Nayler GL, Klipstein RH, Underwood SR, Rees RS, Longmore DB. In vivo validation of MR velocity imaging. J Comput Assist Tomogr 1987;11:751–756.
19. van der Geest RJ, Niezen RA, van der Wall EE, de Roos A, Reiber JH. Automated measurement of volume flow in the ascending aorta using MR velocity maps: evaluation of inter- and intraobserver variability in healthy volunteers. J Comput Assist Tomogr 1998;22:904–911.
20. Frayne R, Steinman DA, Ethier CR, Rutt BK. Accuracy of MR phase contrast velocity measurements for unsteady flow. J Magn Reson Imaging 1995;5:428–431.
21. Ley S, Unterhinninghofen R, Ley-Zaporozhan J, Schenk JP, Kauczor HU, Szabo G. Validation of magnetic resonance phase-contrast flow measurements in the main pulmonary artery and aorta using perivascular ultrasound in a large animal model. Invest Radiol 2008;43:421–426.
22. Goo HW, Al-Otay A, Grosse-Wortmann L, Wu S, Macgowan CK, Yoo SJ. Phase-contrast magnetic resonance quantification of normal pulmonary venous return. J Magn Reson Imaging 2009;29:588–594.
23. Powell AJ, Maier SE, Chung T, Geva T. Phase-velocity cine magnetic resonance imaging measurement of pulsatile blood flow in children and young adults: in vitro and in vivo validation. Pediatr Cardiol 2000;21:104–110.
24. Westenberg JJ, Danilouchkine MG, Doornbos J, et al. Accurate and reproducible mitral valvular blood flow measurement with three-directional velocity-encoded magnetic resonance imaging. J Cardiovasc Magn Reson 2004;6:767–776.
25. Cheng CP, Parker D, Taylor CA. Quantification of wall shear stress in large blood vessels using Lagrangian interpolation functions with cine phase-contrast magnetic resonance imaging. Ann Biomed Eng 2002;30:1020–1032.
26. Papathanasopoulou P, Zhao S, Kohler U, et al. MRI measurement of time-resolved wall shear stress vectors in a carotid bifurcation model, and comparison with CFD predictions. J Magn Reson Imaging 2003;17:153–162.
27. Uribe S, Beerbaum P, Sorensen TS, Rasmusson A, Razavi R, Schaeffter T. Four-dimensional (4D) flow of the whole heart and great vessels using real-time respiratory self-gating. Magn Reson Med 2009;62:984–992.
28. Walker PG, Cranney GB, Scheidegger MB, Waseleski G, Pohost GM, Yoganathan AP. Semiautomated method for noise reduction and background phase error correction in MR phase velocity data. J Magn Reson Imaging 1993;3:521–530.
29. Bernstein MA, Zhou XJ, Polzin JA, et al. Concomitant gradient terms in phase contrast MR: analysis and correction. Magn Reson Med 1998;39:300–308.
30. Bock J, Kreher BW, Hennig J, Markl M. Optimized pre-processing of time-resolved 2D and 3D phase contrast MRI data. In: Proceedings of the 16th Annual Meeting of ISMRM, Berlin, Germany, 2007. (abstract 3138).
31. Bland JM, Altman DG. Statistical methods for assessing agreement between two methods of clinical measurement. Lancet 1986;1:307–310.